Journal of Comparative Physiology B
https://doi.org/10.1007/s00360-018-1162-5

ORIGINAL PAPER

Water bicarbonate modulates the response of the shore crab *Carcinus maenas* to ocean acidification

Bastian Maus[1] · **Christian Bock**[1] · **Hans-O. Pörtner**[1,2]

Received: 13 December 2017 / Revised: 2 May 2018 / Accepted: 9 May 2018

Abstract

Ocean acidification causes an accumulation of CO_2 in marine organisms and leads to shifts in acid–base parameters. Acid–base regulation in gill breathers involves a net increase of internal bicarbonate levels through transmembrane ion exchange with the surrounding water. Successful maintenance of body fluid pH depends on the functional capacity of ion-exchange mechanisms and associated energy budget. For a detailed understanding of the dependence of acid–base regulation on water parameters, we investigated the physiological responses of the shore crab *Carcinus maenas* to 4 weeks of ocean acidification [OA, $P(CO_2)_w = 1800$ µatm], at variable water bicarbonate levels, paralleled by changes in water pH. Cardiovascular performance was determined together with extra-(pH_e) and intracellular pH (pH_i), oxygen consumption, haemolymph CO_2 parameters, and ion composition. High water $P(CO_2)$ caused haemolymph $P(CO_2)$ to rise, but pH_e and pH_i remained constant due to increased haemolymph and cellular [HCO_3^-]. This process was effective even under reduced seawater pH and bicarbonate concentrations. While extracellular cation concentrations increased throughout, anion levels remained constant or decreased. Despite similar levels of haemolymph pH and ion concentrations under OA, metabolic rates, and haemolymph flow were significantly depressed by 40 and 30%, respectively, when OA was combined with reduced seawater [HCO_3^-] and pH. Our findings suggest an influence of water bicarbonate levels on metabolic rates as well as on correlations between blood flow and pH_e. This previously unknown phenomenon should direct attention to pathways of acid–base regulation and their potential feedback on whole-animal energy demand, in relation with changing seawater carbonate parameters.

Keywords Crustacean · Bicarbonate · Cardiac MRI · In vivo ^{31}P NMR spectroscopy · Extracellular pH marker · Cardiovascular system

Abbreviations

3-APP	3′-Aminopropylphosphonate
α	Solubility coefficient; level of significance
ADP	Adenosin-5′-diphosphate
AEP	2′-Aminoethylphosphonate
ANOVA	Analysis of variance
ATP	Adenosin-5′-triphosphate
$[B]_T$	Total boron concentration
bpm	Beats per minute
°C	Degree celsius
c	Concentration
Ca^{2+}	Calcium ion
Cl^-	Chloride ion
CO_2	Carbon dioxide
δ	Chemical shift
FLASH	Fast low angle shot
g	Gramm
GABA	Gamma-aminobutyric acid
H^+	Hydrogen ion/proton
h	Hour(s)
HCO_3^-	Hydrogen carbonate/bicarbonate ion
HCl	Hydrochloric acid
K^+	Potassium ion
L	Liter
M	Molar (mol/L)
m	Meter
m	Mass
Mg^{2+}	Magnesium ion

Communicated by G. Heldmaier.

✉ Christian Bock
Christian.Bock@awi.de

[1] Integrative Ecophysiology, Alfred Wegener Institute Helmholtz Centre for Polar and Marine Research, Am Handelshafen 12, 27570 Bremerhaven, Germany

[2] Department of Biology/Chemistry, University of Bremen, 28334 Bremen, Germany

Published online: 23 May 2018

min	Minute(s)
mol	Mol
$\dot{M}O_2$	Metabolic-/respiration rate
MRI	Magnetic resonance imaging
n	Amount of substance; group size
Na^+	Sodium ion
NH_4^+	Ammonium ion
NMR	Nuclear magnetic resonance
O_2	Oxygen
P	Phosphorous
P	(Partial-)pressure; probability
$P(CO_2)_e$	Partial pressure of CO_2 in haemolymph
$P(CO_2)_w$	Partial pressure of CO_2 in seawater
P_i	Inorganic phosphate
pH	$-\log_{10}[H^+]$
pH_e	Extracellular pH
pH_i	Intracellular pH
pH_w	Sea water pH (free scale)
pK_a	$-\log_{10}$ of dissociation constant in an acid–base equilibrium
pK_a'''	pK_a under defined conditions
PLA	Phospho-L-arginine
PSU	Practical salinity unit
ppm	Parts per million
RARE	Rapid acquisition with relaxation enhancement
RMR	Routine metabolic rate
S	Seawater salinity
SID	Strong ion difference
SMR	Standard metabolic rate
SO_4^{2-}	Sulfate ion
T	Tesla
T	Temperature
t	Time
V	Volume
w_f	Wet weight/fresh weight

Introduction

Unabated fossil-fuel burning and deforestation are projected to elevate atmospheric and surface ocean $P(CO_2)$ to values approaching 1000 µatm by the year 2100 (Doney et al. 2009; Meinshausen et al. 2011). The resulting ocean acidification (OA) will lead to an average drop in surface seawater pH of 0.4–0.5 units below present (Wittmann and Pörtner 2013). OA might cause differential physiological responses of individual marine species and thereby affect their interactions at ecosystem level. With elevated water $P(CO_2)$, CO_2 will reach higher levels in extra- and intracellular compartments as well, inducing a respiratory acidosis (Fabry et al. 2008). Maintaining extracellular pH (pH_e) under elevated $P(CO_2)_e$ requires an increase in $[HCO_3^-]_e$, e.g., through (passive) non-bicarbonate buffering combined with a net increase of HCO_3^- through ion-exchange processes (e.g., Pörtner et al. 1998 for the peanut worm *Sipunculus nudus* and; Gutowska et al. 2010 for the squid *Sepia officinalis*; for *Carcinus maenas* and other crustaceans: Appelhans et al. 2012; Spicer et al. 2007; Truchot 1979; Whiteley 2011). A constant pH_e at elevated plasma $[HCO_3^-]$ helps to maintain intracellular pH (pH_i) under hypercapnia, ensuring optimal enzyme functioning. The increase in $[HCO_3^-]$ under increasing $P(CO_2)$ is more effective in compartments with a high non-bicarbonate buffering capacity and a low control pH, such as in the intracellular space. Non-bicarbonate buffer values decline from intracellular, to extracellular to ambient compartments (Pörtner et al. 2004), resulting in a lower stability of pH under the same increased $P(CO_2)$ in this order. Consequently, acid–base relevant ion-exchange processes between ambient water and the extracellular space are of great significance under changing water conditions with potential implications for whole-animal energy demand (see below; Pörtner et al. 2000; Whiteley 2011).

A fall in extracellular pH is compensated for by ion-exchange mechanisms, such as Cl^-/HCO_3^-, Na^+/H^+ exchange, or H^+-ATPase in specialized tissues like the gills (Charmantier et al. 2009; Hu et al. 2016), or to a minor extent, the antennal gland (Wheatly 1985), actively setting new steady-state values for pH_e in animals subjected to OA. Therefore, a metabolic response, the availability of bicarbonate from the surrounding medium or other carbonate sources, such as the exoskeleton (Spicer et al. 2007), may affect the degree of pH compensation and thus a species' tolerance to acid–base disturbances. Rapid establishment of a new steady state with elevated levels of $[HCO_3^-]_e$ and small net pH changes reduces the importance of passive non-bicarbonate buffering under hypercapnia (Whiteley 2011).

Acclimation to OA causes enhanced activity of ion-exchange processes between water and apical membranes and subsequently between internal compartments. Changing contributions of branchial H^+-ATPase and Na^+/K^+-ATPases may translate into shifts in energy turnover and energy allocation (Pane and Barry 2007; Hu et al. 2017). Changes in the activities and capacities of these transporters are difficult to quantify, but energetic implications due to life-style and environment have been discussed with respect to a species' resilience to OA and long-term performance (Pörtner et al. 2000; Pane and Barry 2007; Kreiß et al. 2015; Hu et al. 2016; Michael et al. 2016). Accordingly, a hypercapnia-induced decrease in pH_e led to a reduced rate of aerobic metabolism in *S. nudus* (Reipschläger and Pörtner 1996) by switching from the Na^+/H^+ exchanger to the less energy consuming Na^+-dependent Cl^-/HCO_3^- exchanger (Pörtner et al. 2000). Metabolic depression with oxygen consumption rates ($\dot{M}O_2$) far below standard rates (Fry 1971) is a way to prolong survival during transient exposure to unfavorable conditions (Guppy and Withers 1999). However,

the responses of different marine invertebrates to various degrees of OA are far from uniform: while some active groups, like squid, maintain metabolic rates at minor drops in extracellular pH ($P(CO_2)_w = 4000–6000$ µatm; Gutowska et al. 2008; Gutowska et al. 2010), swimming crabs *Necora puber* and Dungeness crabs *Metacarcinus magister* displayed reduced $\dot{M}O_2$ at fully compensated pH_e (at 33% of controls; $P(CO_2)_w = 3000$ (both species) and 12,000 µatm (*N. puber* only); Hans et al. 2014; Small et al. 2010). Under a less severe $P(CO_2)_w$ increase to 2400 µatm, blue mussels *Mytilus edulis* failed to maintain pH_e, but increased their $\dot{M}O_2$ (1.6-fold), possibly indicating enhanced activities of regulatory mechanisms (Thomsen and Melzner 2010; Thomsen et al. 2010).

The present study set out to investigate acid–base regulatory responses of an intertidal model species, the shore crab *C. maenas* (Linnaeus 1758) from the North Sea, to increased CO_2 levels causing acidified waters. *C. maenas* is an osmoconformer at full-strength seawater and tolerates daily and seasonal fluctuations of different environmental parameters (temperature, salinity, $P(O_2)$, $P(CO_2)$; Henry et al. 2012; Tepolt and Somero 2014). Under OA, the efficiency of pH_e regulation in *C. maenas* is higher with prolonged exposure (Truchot 1979), but mechanistic investigations of acid–base regulation are scarce, with the exception of early studies by Truchot (1981, 1984), and associated whole-animal metabolic responses have not been studied sufficiently.

Water parameters that may influence acid–base regulation include $P(CO_2)_w$, $[HCO_3^-]_w$ and pH_w. $[HCO_3^-]$ and thus carbonate alkalinity are the main components of total alkalinity (TA; Truchot 1984). To investigate the influence of various parameters of the water carbonate system on acid–base and metabolic regulation, we exposed shore crabs to normocapnia and environmental hypercapnia [i.e., OA with $P(CO_2)_w = 1800$ µatm] in water at control $[HCO_3^-]_w$ compared to acidified water with $[HCO_3^-]_w$ set to 50% of control levels. Animals were exposed to treatment conditions for 4 weeks until experimentation. Exposing crabs to 50% lower $[HCO_3^-]_w$, under both normocapnia and hypercapnia also allowed for assessing the influence of variable levels of water pH (through changes in water bicarbonate levels) on acid–base and metabolic regulation. Combining $\dot{M}O_2$ measurements, in vivo ^{31}P-NMR spectroscopy, cardiac magnetic resonance imaging (MRI) and haemolymph ion quantification in each individual, our goal was to link metabolic rates to energy consuming processes, such as ion regulation, cardiovascular performance, and tissue energy status. Accordingly, we present effects of ocean acidification on the metabolic and cardiovascular response as well as ion- and acid–base regulation of *C. maenas* and analyze to what extent responses are related to water bicarbonate levels.

Materials and methods

Animal collection and incubation

Carcinus maenas were collected from shrimp trawls at the back barrier tidal flats of the island of Spiekeroog (North Sea, NW Germany, 53°44′27.8″N 7°44′35.7″E, depth less than 10 m) in October 2014. Crabs were kept submerged in recirculating seawater aquaria at the Alfred Wegener Institute, Bremerhaven at the in situ temperature = 8 °C, salinity ≈ 33 until the beginning of incubation in March 2015. Animals were fed twice a week ad libitum with frozen cockles. Excess food and feces were regularly removed from the aquaria. Fresh weight (w_f) of the crabs ranged from 21 to 66 g, corresponding to a carapace width of 3–6 cm. Specimens with similar size distributions were used in all experimental groups. Mean body weight was around 35 g and not significantly different between groups. In total, 23 male, intermolt green crabs were used for experiments. Each individual was subjected to the same set of measurements.

During incubation, animals were kept submerged in 50 L seawater aquaria in a temperature controlled room ($T_w = 8.0–8.5$ °C) and exposed to the following conditions for 4 weeks prior to any experiments (see Table 1): control, with ambient $P(CO_2)_w$ and pH_w; OA, with

Table 1 Water parameters of incubation media

Group	Group size (n)	T_w (°C)	S (PSU)	$P(CO_2)_w$ (µatm)	$[HCO_3^-]_w$ (mM)	pH_w	$[H^+]_w$ (nM)	Total alkalinity (mM)	DIC (mM)
Control	7	8.24 ± 0.47^{ab}	32.84 ± 0.93	440 ± 37^{a}	2.21 ± 0.25^{a}	8.12 ± 0.04^{a}	7.67 ± 0.73^{a}	2.57 ± 0.21^{a}	2.39 ± 0.19^{a}
OA	6	8.46 ± 0.09^{a}	32.76 ± 1.16	1820 ± 64^{b}	2.24 ± 0.14^{a}	7.50 ± 0.03^{b}	31.40 ± 2.29^{bc}	2.33 ± 0.15^{b}	2.36 ± 0.14^{a}
Low $[HCO_3^-]_w$	6	8.27 ± 0.13^{ab}	32.60 ± 1.04	390 ± 55^{a}	1.08 ± 0.16^{b}	7.85 ± 0.05^{c}	14.32 ± 1.56^{ab}	1.17 ± 0.17^{c}	1.11 ± 0.16^{b}
OA + low $[HCO_3^-]_w$	4 + 1 ♀	8.24 ± 0.12^{b}	32.84 ± 1.05	1820 ± 53^{b}	1.10 ± 0.18^{b}	7.19 ± 0.07^{d}	65.39 ± 10.55^{c}	1.11 ± 0.17^{c}	1.18 ± 0.16^{b}

Values are group means ± standard deviation of the weekly measurements of the parameters. While part of the incubation, the one female under OA + low $[HCO_3^-]_w$ was not used in the analysis. Different letters denote statistically significant differences between groups in the respective parameter. Salinities were not different among groups

$P(CO_2)_w = 1800$ µatm, resembling strong, next century OA conditions (see "Introduction"); low $[HCO_3^-]_w$ reduced to 50% of control through the molar addition of HCl and checked by measurements of water $P(CO_2)$ and pH, see below; and OA + low $[HCO_3^-]_w$. Individuals were kept in cages (PVC mesh). The incubation system per group consisted of a 500 L main tank, a header tank, two aquaria, and an overflow basin (~ 790 L in total). The water of the normocapnic groups was aerated with compressed air, while OA and OA + low $[HCO_3^-]_w$ were aerated with an air/CO_2-mix, set by a gas-mixing device (HTK Hamburg GmbH, Germany). Seawater of the respective main tanks was exchanged once per week in every group.

Water temperature, salinity, $P(CO_2)_w$, and pH_w (free scale) were measured once a week in each aquarium and in supply tanks of the in vivo experiments before introducing the animals. Temperature and salinity were measured directly in the aquaria with a conductivity meter (LF197, WTW, Weilheim, Germany). $P(CO_2)_w$ was determined from the gas phase of the seawater with a combined carbon dioxide probe (CARBOCAP GMP343, Vaisala, Helsinki, Finland) and carbon dioxide meter (CARBOCAP GM70, Vaisala). The pH meter (pH3310, WTW) was calibrated with NIST buffers (pH 6.865 and 9.180) at the incubation temperature. Seawater pH was determined in 50 mL sub-samples covered with parafilm to minimize gas exchange. pH_w was transferred to the free scale, with corrections for T_w, ionic strength and a reference buffer-pH in artificial seawater (Waters and Millero 2013), as recommended by Dickson (2010). $[HCO_3^-]_w$ was calculated through "CO2Sys" (v2.1, Pierrot et al. 2006), with K_1 and K_2 from Millero (2010), KSO_4 from Dickson (1990), and $[B]_T$ from Uppström (1974).

Reductions in water bicarbonate levels will always be accompanied by reductions in water pH at a given $P(CO_2)_w$ (see Table 1). Compared to control values of pH_w 8.12 ± 0.04, OA induced by CO_2 led to pH_w of 7.50 ± 0.03, 0.35 units lower than under normocapnia and low $[HCO_3^-]_w$. However, the lowest pH_w was found under OA + low $[HCO_3^-]_w$ (7.19 ± 0.07).

Respirometry

Metabolic rates in undisturbed, unrestrained crabs were calculated from oxygen consumption measurements ($\dot{M}O_2$) after 4 weeks of exposure to experimental conditions, following recommendations by Steffensen (1989) and Dupont-Prinet et al. (2010). Briefly, individuals were placed in a respiration chamber ($V_{chamber} = 1720$ mL), which in turn was submerged in a covered tank of 40 L seawater at the respective experimental conditions. Feeding was stopped at least 48 h before respirometry (McGaw and Penney 2014). Baseline $\dot{M}O_2$ was recorded as standard metabolic rate (SMR) and phases of spontaneous activity were identified as peaks in metabolic rate (spMR; see statistics for further details; Brand 1990; Fry 1971; Klein Breteler 1975).

Respiration chambers were designed to be perfused by intermittent flow and the water surrounding the chambers was permanently aerated with the respective air-CO_2-mix (see above). The oxygen content was measured as percent air saturation, once every 1–5 min with a temperature compensated fiber-optical oxymeter (FIBOX 3; PreSens, Regensburg, Germany) using software PSt3 (v7.01, PreSens). Clock timers controlled periodic activation of one flush pump per respirometer. Flushing lasted for 15 min per hour at a rate of 300 L h^{-1}. When closed, the re-circulation was continuously active at 490 L h^{-1} (Eheim aquarium pumps, Deizisau, Germany). Oxygen sensors were calibrated before each run by flowing N_2 gas at 0% O_2 and within the fully aerated closed circulation at 100% air saturation. One set of measurements lasted 48 h.

The ratio of animal volume to chamber volume was 0.01–0.05 for all crabs. Respirometers were wiped with 70% ethanol and rinsed with deionized water to reduce contamination with aerobic microorganisms after each run: blank measurements before and after any run showed declines in oxygen saturation of less than 1% h^{-1} over a period of 5 h, respectively.

Weight-specific oxygen consumption of crabs ($\dot{M}O_2$ in nmol min^{-1} g^{-1}) was calculated from

$$\dot{M}O_2 = c_{O_2} \cdot (V_{chamber} - V_{ind.}) \cdot \frac{\Delta c_{sat.}}{\Delta t \cdot w_f \cdot 100}, \quad (1)$$

with $\Delta c_{sat.} \cdot \Delta t^{-1}$ as the recorded change in oxygen saturation over time (percent per minute). c_{O_2} represents water oxygen concentration at full saturation under the given atmospheric pressure, using a_{O_2} (solubility coefficient; µM $Torr^{-1}$) provided by Boutilier et al. (1984) and P_{wv} (vapor pressure of water) by Dejours (1981). Mean oxygen saturation changes over time were calculated in LabChart Reader (v8.0.5, ADInstruments, Oxford, UK). Each value of $\dot{M}O_2$ represents a 45-min average.

MR imaging and spectroscopy

Individuals recovered for 1 week after $\dot{M}O_2$ measurements and were then subjected to interlaced in vivo ^{31}P-NMR and MRI measurements in a horizontal 4.7 T MRI scanner with 40 cm bore (47/40 Biospec AVANCE III; Bruker BioSpin GmbH, Ettlingen, Germany). Changes in tissue cellular energy status, pH_e and pH_i were investigated using in vivo ^{31}P-NMR spectroscopy. Cardiovascular activity was investigated using self-gated cardiac MRI together with phase contrast MRI for the quantification of haemolymph flow (Bock et al. 2012). Individuals were kept in a sealed chamber of ~ 300 mL volume, that was constantly perfused with

seawater at the respective incubation conditions similar to Bock et al. (2001a, b). The chamber was placed under a ^{1}H-, ^{13}C-, ^{31}P-tunable 50-mm-diameter surface coil, centered above the animal. The animals could move their legs, but were laterally restricted by levers to keep the carapace in a permanent position, checked by three perpendicularly oriented MR overview images (pilot scans). Animals were allowed to recover from potential handling stress for at least 1 h, verified by repeated ^{31}P-NMR spectra (see below). Total time in the magnet was 8–16 h for each animal.

Simultaneous measurements of pH_i, pH_e, and energy status

Changes in pH and bioenergetics were studied by in vivo ^{31}P-NMR spectroscopy (Pörtner et al. 2010). Intra- and extracellular pH were determined simultaneously. 3-Aminopropylphosphonate (3-APP) was used as an extracellular pH indicator, as shown in rats (Gillies et al. 1994), and applied to crustaceans for the first time. Preliminary studies showed no toxic effects of 3-APP and constant signal intensity over several weeks (Kreiß 2010). A solution of 250 mM 3-APP was prepared to represent the ionic composition of the haemolymph of *C. maenas* (Kreiß 2010). The solution was injected after the respiration experiments through the articular membrane between the coxa and the basis of the third, right walking leg to a final [3-APP] of ~ 10 mM in the animal. Assuming a haemolymph volume of one-third of fresh body weight, the injected volume was always around 8% of the body volume of a crab. No buffer was added to the solution to not disturb the haemolymph buffering system. The crabs were allowed to recover from the injection for 5 days under their respective incubation conditions (Table 1) before being subjected to NMR experiments. Individual respiration measurements found no side effects of 3-APP on the metabolic rate of *C. maenas*.

Injection of 3-APP did not change SMR under control conditions, nor did it affect mortality or general animal behavior during the incubation (visual observation and feeding success). The 3-APP signal was clearly detectable in the spectra for several weeks with a sufficiently high peak surface area to determine pH_e, indicating no dilution or degradation of the marker in *C. maenas*. High-resolution ^{31}P-NMR spectra of haemolymph samples extracted after the experiments displayed only one distinct signal peak at the chemical position of 3-APP which varied with the pH of the haemolymph sample. The peak areas changed with the 3-APP concentration injected into the crab (data not shown). It can thus be concluded that the chemical shift of 3-APP ($\delta_{3\text{-APP}}$) is indeed indicative of haemolymph pH.

For studies of intracellular pH surface, coils produce a hemispheric excitation profile in NMR spectroscopy and have the advantage that the localization is limited to this profile, which makes the assignment of NMR signals to a specific tissue easier, compared to more homogenous excitation profiles produced by volume coils. In this study, we used a surface coil of 5-cm diameter positioned dorsally above the heart. Its excitation profile covers a maximum volume of ~ 33 cm^3 with the heart in its center. While this excitation volume will be further reduced by the conductive properties of seawater (e.g., Bock et al. 2002), it can be assumed that the high-energy phosphate signals—including P_i—mainly identified cardiac muscle pH_i, and to a lesser extent that of surrounding tissue, including gills and hepatopancreas/gonads, while the 3-APP signal originated from the haemolymph.

In vivo ^{31}P-NMR spectra were collected as described for marine organisms by Bock et al. (2002) (parameters: TR: 1400 ms; pulse bp32, 200 µs; flip angle: 60°; 400–1600 averages) and processed with Topspin 3.0 (Bruker BioSpin GmbH, Rheinstetten, Germany) using a software routine (CTjava, AWI, R. Wittig, personal communication): ^{31}P-NMR signals of P_i, 3-APP and phospho-L-arginine (PLA) were picked automatically and fitted to a Lorentz distribution through a least-square method (mdcon, Bruker BioSpin, Rheinstetten), briefly described by Bock et al. (2001b). The parameters of the respective Lorentz distributions were used to calculate the chemical shift ($\delta_{PLA} = 0$ ppm), from which pH values were then calculated according to Kreiß (2010), applying constants derived at 10 °C. For P_i: $pK_a = 6.79$; $\delta_{min} = 4.24$ ppm; $\delta_{max} = 6.59$ ppm (modified after Zange et al. 1990). For 3-APP: $pK_a = 7.11$; $\delta_{min} = 24.1275$ ppm; $\delta_{max} = 27.6275$ ppm (after Gillies et al. 1994). The equations are as follows:

$$pH_e = pK_{a\,3\text{-APP}} - \log\frac{\delta - \delta_{min}}{\delta_{max} - \delta}, \quad (2)$$

$$pH_i = pK_{a\,P_i} + \log\frac{\delta - \delta_{min}}{\delta_{max} - \delta}. \quad (3)$$

In addition to the calculation of pH, the PLA/P_i ratio, an index of cellular energy status, was calculated from peak surface areas of PLA and P_i (cf. Gutowska et al. 2010; Sokolova et al. 2000). While pH_i and pH_e remained at their respective control levels under all applied experimental treatments, changes of pH_i and pH_e were observed after short periods of hypoxia in a separate experiment (data not shown), confirming the applicability of this technique to observe pH fluctuations. Values of pH_i (averaging heart muscle, gills, and hepatopancreas/gonads) and pH_e are given as means of at least 10 consecutively acquired ^{31}P-NMR spectra per animal (maximum: 50 spectra), excluding the first hour of measurement after the animals were placed in the magnet.

Determination of cardiovascular performance

Alternating with spectroscopy, cardiovascular performance was determined using flow-weighted MRI as described by Bock et al. (2001a, see below) and a self-gated cardiac cine MRI sequence to determine heart rate and heart function (Bock et al. 2012; Bohning et al. 1990, IntraGate©, Bruker BioSpin GmbH, Ettlingen; method: IntraGateFLASH; TR: 8.0 ms; TE: 3.051 ms; 128 averages; flip angle: 45°; attenuation: 13.6 dB; matrix size: 256×256; FOV: 6×6 cm^2). The slice position was based on anatomical imaging, namely, packages of horizontal slices from fast spin-echo MRI using RARE (rapid acquisition with relaxation enhancement; TR: 3 s; TE: 69.6 ms; 2 averages; flip angle: 180°; matrix size 256×256; FOV: 6×6 cm^2). From each 2-min scan, a 20-s period with periodic raw signals was selected, the signal peaks were counted, and heart rate was calculated in beats per minute (bpm).

Blood flow was quantified in the arteria sternalis from coronal cross sections using phase-contrast, flow-weighted MRI. This technique quantifies the velocity of moving hydrogen atoms (usually from water/blood) under directed flow conditions (Pope and Yao 1993, method: FLOWMAP; TR: 25.104 ms; TE: 12.0 ms; 16 averages; flip angle: 30°; attenuation: 20 dB; matrix size: 512×256; FOV: 6×6 cm^2; flow encoding: slice direction; v_{min}–v_{max}: 0.3–12.0 cm s^{-1}). The arteria sternalis supplies haemolymph to the walking legs (McGaw et al. 1994). The rhythmic flow in the arteria sternalis was used for quantification of the heart rate within IntraGate when a direct visualization of heart contractions failed. Through integrated macros in the software Paravision 5.1 (Bruker BioSpin GmbH, Ettlingen), a region of interest was manually fitted to the artery and the included phase information was transformed into flow velocity.

Cardiac and blood-flow MR imaging were conducted in blocks together with ^{31}P-NMR spectroscopy, resulting in a scan time of 15 min per block. Blocks were repeated over the entire experimental time course for each individual (8–16 h). At least three values (from three separate scans) were analyzed for heart- and flow rate evenly distributed over the entire time course to account for potential inter-individual variations.

Anatomical and flow-weighted MR images resulted in a similar quality as reported previously for bigger decapod crustaceans (Fernández et al. 2000; Bock et al. 2001a). Self-gated cardiac cine MRI yielded similar heart rates as shown recently for *Cancer pagurus* (Bock et al. 2012). Heart rates under control conditions were comparable to those reported for similar-sized crabs and similar T_w, determined using Doppler sensors (Frederich and Pörtner 2000; Walther et al. 2009; Wittmann 2010). In addition, by use of phase-contrast MRI, blood-flow rates in the arteria sternalis of *C. maenas* were well in accordance with literature data (Belman 1975).

Analysis of haemolymph

After at least 5 days of recovery from the in vivo experiments, haemolymph samples were removed with an ice-cold syringe from the base of one of the walking legs that was not previously used for injections. If possible, two 200-µL sub-samples were taken from the total haemolymph sample (≤ 500 µL), extracted with a gas-tight glass syringe and injected into two septum-sealed glass flasks, containing 3-mL 0.1 M HCl each. Flasks were used for duplicate measurement of total CO_2 concentration [$c(CO_2)$] through gas-phase chromatography (G6890N, Agilent Technologies, Santa Clara, USA), with readings < 5% different between duplicates. The remaining volume (~ 100 µL) was transferred to 0.5-mL Eppendorf tubes and stored at − 20 °C for the analysis of ion composition (see below).

Standards were established by dilutions of a CO_2 solution (1-g CO_2/L, Reagecon, Shannon, Ireland) and measured in duplicates. Blanks, accounting for the residual CO_2 in the air and HCl, were measured in duplicate through the addition of 200-µL milliQ water. The area of the respective peak represented the sample $c(CO_2)_e$. $P(CO_2)_e$ and $[HCO_3^-]_e$ were calculated according to Heisler (1986) and Pörtner et al. (1990) using values of CO_2 solubility coefficient α and apparent first dissociation constant pK_a''' calculated after Heisler (1986):

$$P(CO_2)_e = \frac{c(CO_2)_e}{10^{pH_e - pK_a'''} \cdot \alpha + \alpha}, \quad (4)$$

$$[HCO_3^-]_e = P(CO_2)_e \cdot \alpha \cdot 10^{pH_e - pK_a'''}. \quad (5)$$

To estimate which ion-exchange processes are associated with acid–base regulation under the different acidified conditions, we analyzed the concentrations of Na^+, K^+, Mg^{2+}, Ca^{2+}, and Cl^- through ion chromatography (ICS1500 for cations and ICS2000 for anions, Dionex, Sunnyvale, USA) in the remaining haemolymph as described by Wittmann (2010). A conductivity cell and a self-regenerating suppressor at 32 mA were used to reduce background noise. Cations were separated on an IonPac CS16 (Dionex, Sunnyvale) column with 30-mM methane-sulphonic acid as an eluent. An IonPac CG16 column was used as a guard to pre-filter the sample solution and to avoid overloading of the actual analytical column. The flow rate was 0.36 mL min^{-1} at a temperature of 40 °C. Combined Six Cation Standard-II (Dionex) was used to quantify the concentration in mM. Haemolymph samples were measured after 1:300 dilution with milliQ water. Anions were measured after 1:2100 dilution, using the diluted samples prepared for cation analyses. The reference standard was Combined Five Anion Standard (Dionex). Anions were separated on an AS11-HC analytical column, with an IonPac AG-11 as guard column. The suppressor current intensity for anions was 23 mA. 30-mM

KOH was used as eluent, at a flow rate of 0.30 mL min^{-1}. The column- and cell temperature was 30 °C. All samples were randomly measured.

Statistics and data analysis

The 15% percentiles were derived from the recordings of $\dot{M}O_2$. The mean of the lowest 15% of values was assumed to represent SMR, while the mean of the highest 15% was defined as spMR during phases of spontaneous activity. This way, biological variability is accounted for (Dupont-Prinet et al. 2010). Outliers are defined as those values smaller (for SMR) or larger (for spMR) than the mean of the 15% percentiles ± two times the standard deviation. Consequently, we calculated (absolute) spontaneous aerobic scope as spMR–SMR and factorial spontaneous scope as $spMR \cdot SMR^{-1}$ (Clark et al. 2013).

All data per incubation group were checked for normal distribution (Shapiro–Wilk test) and equal variance (Levene's test). Outliers within groups were identified through Grubb's test at $\alpha = 0.05$. The number of animals n is given in all tables and figures. ANOVA with Student–Newman–Keuls post-hoc test at $\alpha = 0.05$ identified statistically significant differences between groups. Non-parametric tests (Kruskal–Wallis ANOVA on ranks with Dunn's post-hoc test) were used in case of non-normal distribution or non-equal variance. Correlation among physiological parameters of all experimental animals was assessed through Spearman's rank correlation coefficient ($\alpha = 0.05$). All results are given as group mean ± standard deviation. All statistical analyses were conducted with SigmaPlot 12.0 (Systat Software, 2010).

Results

Incubation and water parameters

$P(CO_2)_w$ and pH_w were set according to experimental conditions and, together with unchanged salinity and T_w, were kept more or less constant during experimentation (Table 1). A transient depression of pH_w from 8.13 to 8.02 and $[HCO_3^-]_w$ from 2.2 to 1.6 mM was found in the control group 2 weeks after the NMR experiments and 4 weeks before haemolymph sampling, for unknown reasons. This depression was reversed within 1 week through a double exchange of water and assumed to remain without consequences for later results. Significant differences in $P(CO_2)_w$ were found between normocapnic groups and OA groups, as well as in $[HCO_3^-]_w$ and DIC for groups with control and low water bicarbonate levels. Total alkalinity was higher under control $[HCO_3^-]_w$, compared to low $[HCO_3^-]_w$, by more than 1.2 mM. TA in the control group was also higher than under OA, by about 0.2 mM. All treatments showed significantly different water pH values. While temperatures were slightly but significantly different between groups, mean values differed only by up to 0.2 °C over the entire incubation time. One out of eight animals died in each normocapnic and two out of seven animals in each hypercapnic group. Grubb's test revealed one outlier under control and OA conditions.

Metabolic rates

Continuous 48 h recordings of rates of oxygen consumption usually showed phases of relatively low values, interrupted by periods of spontaneous activity, and exemplified for one animal from the control group in Fig. 1. Initially, high $\dot{M}O_2$ turned into more stable baseline values and interspersed with spontaneous activity bouts, after approximately 15–20 h in all groups.

Figure 2a shows standard metabolic rates (SMR) and spontaneous metabolic rates (spMR) of the different groups. SMR did not deviate significantly from control values (10.55 ± 0.89 nmol min^{-1} g^{-1}, Fig. 2a) under any experimental treatment. However, the SMR under OA conditions (group 1) of 13.24 ± 3.23 nmol min^{-1} g^{-1} was significantly higher than the SMR found at both low $[HCO_3^-]_w$ and at OA + low $[HCO_3^-]_w$, at rates of 8.68 ± 2.97 and 9.17 ± 2.53 nmol min^{-1} g^{-1}, respectively. These differences were even more pronounced during phases of spontaneous activity: OA alone led to a significantly increased spMR of 48.62 ± 7.05 nmol min^{-1} g^{-1}, compared to 27.66 ± 5.06 nmol min^{-1} g^{-1} under OA + low $[HCO_3^-]_w$ (group 3). The spMR under OA + low $[HCO_3^-]_w$ was the lowest among all treatments, being significantly lower than the control spMR of 40.67 ± 5.79 nmol min^{-1} g^{-1}.

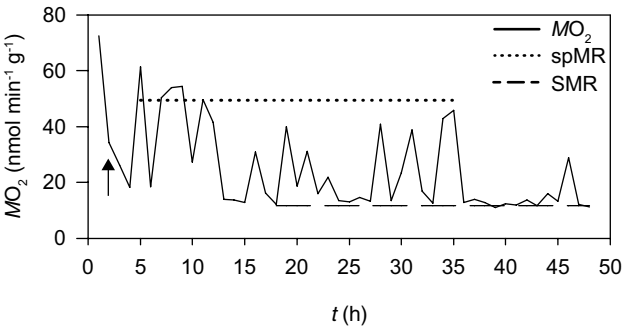

Fig. 1 Example of a time series of recorded metabolic rates ($\dot{M}O_2$). Data points represent the mean decline of saturation for 1 h, derived from an animal under control conditions. Mean SMR, representing mean of lowest 15%; mean spMR, representing mean of highest 15% of all data points, excluding the first hour. The arrow thus marks the beginning of the analysis

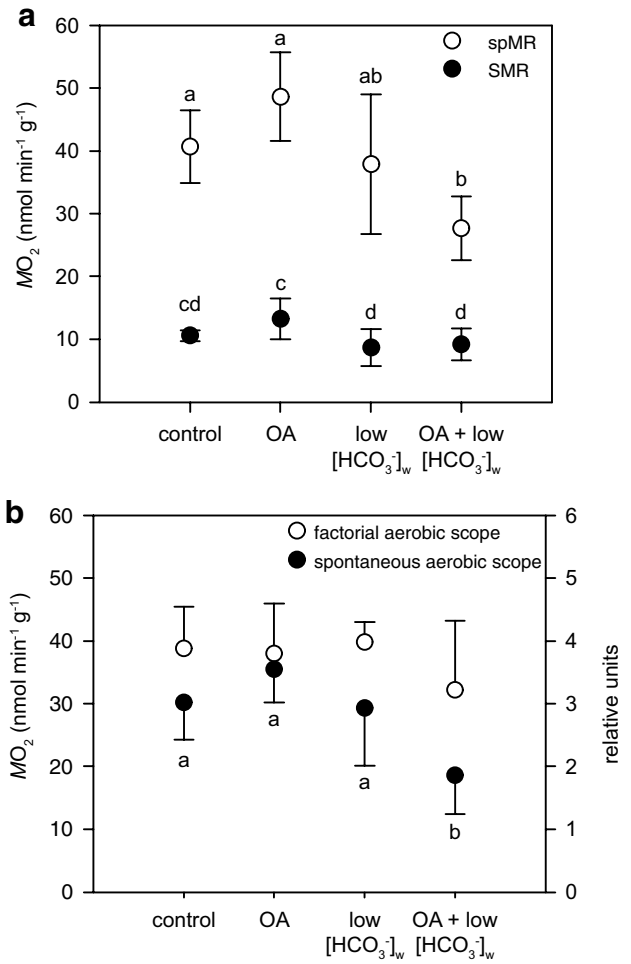

Fig. 2 Metabolic rates and aerobic scope under differently acidified water conditions. **a** Metabolic rates under standard conditions and during spontaneous activity bouts. **b** Absolute routine aerobic scope (filled circles; spMR–SMR) and factorial aerobic scope (open circles; spMR·SMR^{-1}). Control: $n=7$; OA: $n=5$; low $[HCO_3^-]_w$: $n=6$; OA + low $[HCO_3^-]_w$: $n=4$. $T_w=8$ °C. Data points are means ± SD. Different letters indicate significant differences (ANOVA, $P<0.05$) for spontaneous aerobic scope only

Accordingly, animals under OA + low $[HCO_3^-]_w$ showed the smallest spontaneous net aerobic scope, which was significantly reduced compared to all other groups (Fig. 2b). However, factorial spontaneous aerobic scopes were not significantly different between experimental groups (Fig. 2b) in line with a reduced SMR at low $[HCO_3^-]_w$.

Cardiac performance

Figure 3a–c shows an example of coronal MRI scans, selected for blood-flow and heart-rate determinations. The animal is oriented with its mouth (anterior) to the left. The arteria sternalis is visible in the center of the image and was easily identifiable in all animals (arrow). Gill chambers and the ventilatory water movements therein are visible laterally on both sides of the animal (top and bottom of Fig. 3a–c). Blood flow, quantified from phase-contrast MR images of different vessels, was in the range of < 1–5 cm s^{-1} depending on vessel location and size. Mean heart rate was found to be constant at about 48 bpm under all conditions (Fig. 3d) and blood flow under OA was not significantly different from that under control conditions. However, blood-flow rates at both low $[HCO_3^-]_w$ and at OA + low $[HCO_3^-]_w$ were significantly lower than under OA alone (Fig. 3e, as exemplified in Fig. 3c). Blood flow decreased by almost 1 cm s^{-1} from 3.42 ± 0.20 cm s^{-1} under OA to 2.45 ± 0.49 cm s^{-1} under OA + low $[HCO_3^-]_w$.

Tissue and haemolymph acid–base parameters

Figure 4a presents a typical in vivo ^{31}P-NMR spectrum, with the major phosphorus compounds of the animal, such as the three signals of ATP (γ-, α-, and β-ATP), phospho-L-arginine (PLA, taken as internal standard), free inorganic phosphate (P_i) and aminoethyl-phosphonic acid (AEP), a natural compound exclusively found in male crabs (Kleps et al. 2007). In addition, the signal of injected 3-APP was visible around 25 ppm and confirmed to show no interference or overlap with endogenous phosphorous compounds. Mean pH_i or pH_e values were similar in all groups (Fig. 4b): pH_i—determined from the P_i signal—was found to be close to 7.20 ± 0.08 throughout. pH_e—calculated from the position of the 3-APP signal—was 7.86 ± 0.06 in the control group and close to 7.79 ± 0.09 under OA + low $[HCO_3^-]_w$. The concentration of PLA in relation with P_i (approximated from signal peak areas) was elevated under OA + low $[HCO_3^-]_w$, but the increase was only significant compared to control conditions (Fig. 4c). All experimental animals displayed stable pH_e and pH_i values during the entire period of the NMR experiments.

Figure 5 shows the interdependent levels of $[HCO_3^-]_e$, $P(CO_2)_e$, and pH_e in a pH-bicarbonate diagram of the haemolymph of *C. maenas*. A $P(CO_2)_e$ of 0.38 ± 0.09 kPa was found under control conditions, and similar to low $[HCO_3^-]_w$ under normocapnia. High water $P(CO_2)$ led to a significant increase in $P(CO_2)_e$ and $[HCO_3^-]_e$ at unchanged pH_e, compared to the normocapnic groups. Under hypercapnic incubation, $P(CO_2)_e$ nearly doubled to 0.68 ± 0.20 kPa (OA) and 0.65 ± 0.25 kPa (OA + low $[HCO_3^-]_w$). A 50% increase was found for $[HCO_3^-]_e$. Conversely, reductions in seawater bicarbonate concentrations only led to minor, insignificant declines in the respective haemolymph concentrations under either hyper- or normocapnic incubations. Note that the values for groups OA and OA + low $[HCO_3^-]_w$ are elevated above the non-bicarbonate buffer line in the pH-bicarbonate diagram, indicating compensation of the acidosis by a net increase of $[HCO_3^-]$ (Fig. 5).

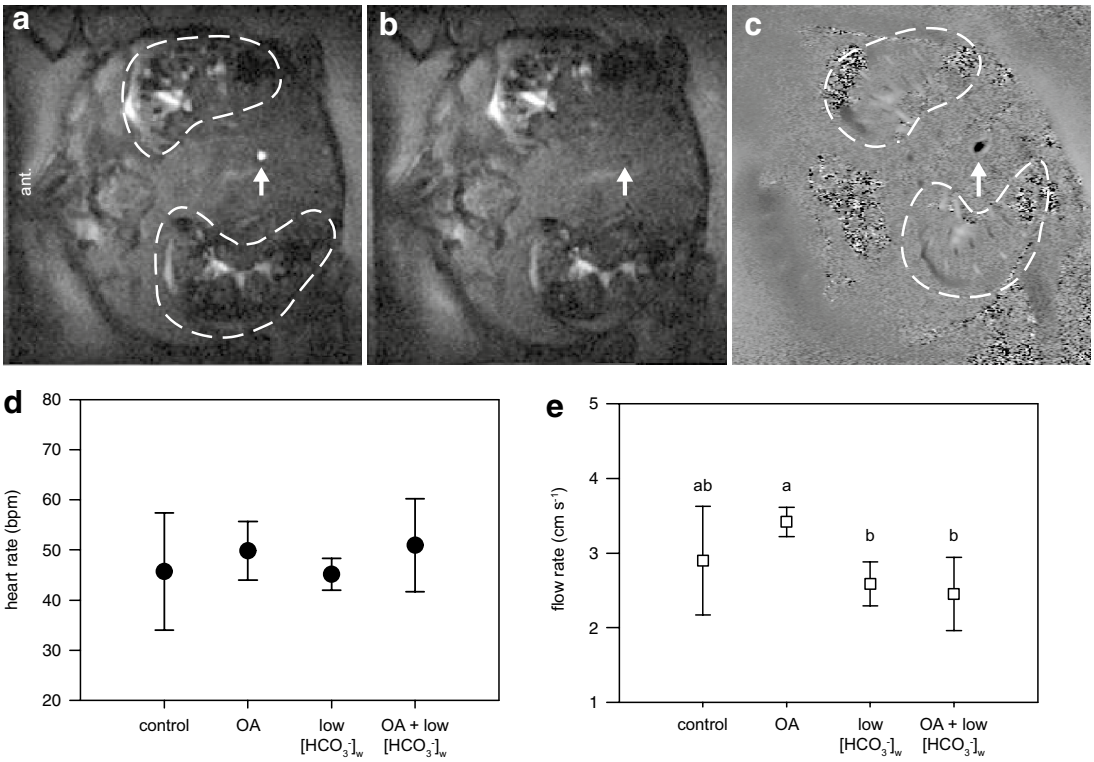

Fig. 3 MRI of the circulatory system, heart rate, and haemolymph flow rate. **a** IntraGateFLASH MRI, showing systolic and diastolic (**b**) phases of blood flow in the arteria sternalis (white arrow). Dorsal view, anterior facing left in the image. **c** Phase-contrasted, flow-encoded MRI. Bright or dark coloring indicates directed flow. Note the visibility of the lateral gills (dashed white lines). **d** Mean heart rate and **e** haemolymph flow rate. Control: $n=5$; OA: $n=5$; low $[HCO_3^-]_w$: $n=6$; OA + low $[HCO_3^-]_w$: $n=4$. $T_w=8$ °C. Data points are means ± SD. Different letters indicate significant differences (ANOVA, $P<0.05$)

Ion composition of the haemolymph

An increase of cations above control levels was found in all experimental groups, and the highest concentrations were seen under OA + low $[HCO_3^-]_w$ (Table 2). This increase is mainly due to increased Na^+ and Mg^{2+} concentrations. All treatments showed significantly higher $[Mg^{2+}]$ compared to control conditions; however, differences in $[Mg^{2+}]$ remained insignificant between experimental treatments. While the increase of $[Ca^{2+}]$ under OA and OA + low $[HCO_3^-]_w$ was significant, compared to the two normocapnic groups, the absolute difference was less than 2 mM. K^+ concentrations remained constant in all groups, at average levels of ~ 13 mM.

Ocean acidification did not affect haemolymph $[Cl^-]$ in the same way as it affected $[Na^+]$ (Table 2): while $[Na^+]$ increased significantly in both absolute and relative terms, $[Cl^-]$ remained at control levels, generally reflecting an increasing strong ion difference (SID) in the haemolymph. Under low $[HCO_3^-]_w$, $[Cl^-]$ was about 110 mM lower than $[Na^+]$. This $[Cl^-]$ deficiency at low ambient bicarbonate levels was significant compared to control conditions and OA + low $[HCO_3^-]_w$. Animals under OA + low $[HCO_3^-]_w$ showed the highest mean concentration of Cl^- and marginally the highest total ion concentration of 1080 ± 45 mM; however, these values were not significantly different from controls. Only under OA + low $[HCO_3^-]_w$ were both $[Na^+]$ and $[Cl^-]$ increased; however, these changes were not significant for $[Cl^-]$.

Correlation of acid–base and functional parameters

Comparing individuals from all treatments, there was a significant positive correlation between spMR and SMR (Fig. 6a), as suggested by a constant factorial scope (Fig. 2b). However, only the spMR was also significantly correlated with blood-flow rates in the arteria sternalis, while the SMR was not (Fig. 6b, c). Furthermore, $[HCO_3^-]_e$ showed a significant, positive correlation with blood-flow rates (Fig. 6f).

Under control $[HCO_3^-]_w$, increased pH_e values were correlated with reduced SMR, spMR, and blood flow. However, only the negative correlation between blood flow and pH_e was significant. In animals incubated at low $[HCO_3^-]_w$ spMR or SMR were hardly related to pH_e (Fig. 6g, h)—while the blood-flow pH_e correlation had even turned positive (flow increased with increasing pH_e; Fig. 6i).

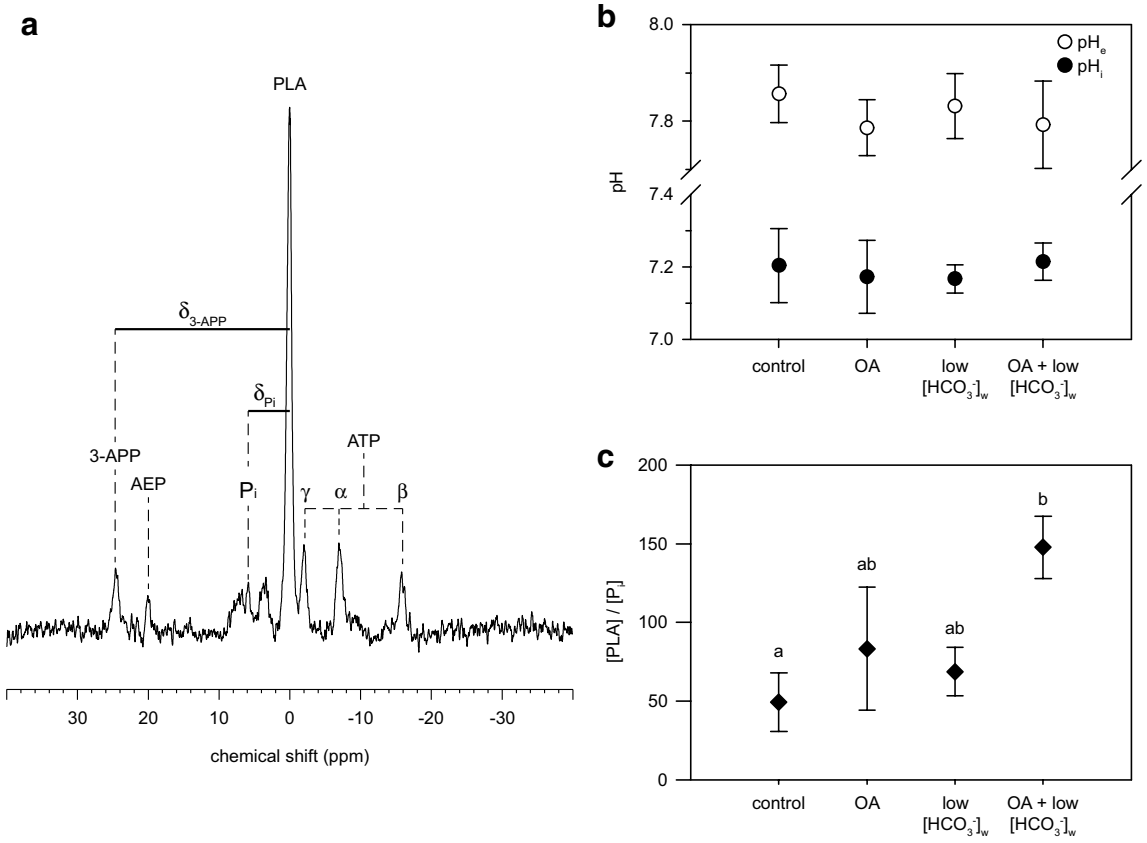

Fig. 4 ^{31}P-NMR spectrum, used to derive pH_i, pH_e and intracellular energy status. **a** In vivo whole-animal ^{31}P-NMR spectrum of a male *C. maenas*. Peaks are labeled as follows: *3-APP* 3-aminopropylphosphonate, *AEP* 2-aminoethylphosphonate, *P_i* inorganic phosphate. *PLA* phospho-L-arginine, *ATP* adenosine triphosphate, with α, β and γ phosphates as distinct peaks. Values for pH_i and pH_e were calculated from the chemical shift between PLA and P_i (δ_{Pi}) and 3-APP ($\delta_{3\text{-APP}}$), respectively. **b** Mean pH_i and pH_e, derived from whole-animal in vivo ^{31}P-NMR spectra. Intracellular pH is representative for gills, cardiac muscle, and hepatopancreas/gonads. **c** Ratio of the concentrations of PLA over P_i. Control: $n = 6$; OA: $n = 5$; low $[HCO_3^-]_w$: $n = 6$; OA + low $[HCO_3^-]_w$: $n = 4$. $T_w = 8$ °C. Data points are means ± SD. Different letters indicate significant differences (ANOVA on ranks, $P < 0.05$)

Discussion

This study aimed to explore the medium-term (4 weeks) effects of key parameters of seawater physicochemistry (pH, $P(CO_2)$, $[HCO_3^-]$) on energy demand, acid–base, and ion regulation of the shore crab *C. maenas*. Statistical analyses confirmed that the desired treatment conditions (especially $P(CO_2)_w$ and $[HCO_3^-]_w$) were significantly different between the respective groups. We found that metabolic rates, spontaneous activity, blood flow, and intracellular energy reserves were differently affected or adjusted by the respective treatments. As a key finding, *C. maenas* was able to compensate for any changes in extra- and intracellular pH that may have occurred initially, under any experimental condition. Mortalities were low and similar across all groups and could be attributed to existing fractures of the exoskeleton. These observations indicate that *C. maenas* is highly resilient to the variable conditions of its intertidal to subtidal habitat. Intermittent flow respirometry at 8 °C found SMRs of ~ 12 nmol min^{-1} g^{-1} under control conditions, in line with earlier results obtained in unfed crabs at similar weight and temperature (7 °C; Robertson et al. 2002). Maintenance or re-establishment of resting state during medium-term exposure was also indicated by the observation that SMRs and cardiovascular activities in experimental groups were not significantly different from control values. In addition, almost constant factorial scopes in all treatments provide evidence for a parallel shift in the standard and spontaneous metabolic rates (Fig. 2b). The largest difference between responses was found under OA versus OA + low $[HCO_3^-]_w$: crabs showed a 40% lower spontaneous activity under OA + low $[HCO_3^-]_w$, when compared to OA at control $[HCO_3^-]$. These findings are corroborated by significantly depressed spMR, SMR, as well as absolute spontaneous scope and haemolymph flow rate under OA + low $[HCO_3^-]_w$ (Figs. 2, 3e). Together with a high PLA/P_i ratio in tissues including muscle, these findings may reflect a relaxation effect in *C. maenas* induced by CO_2, especially at

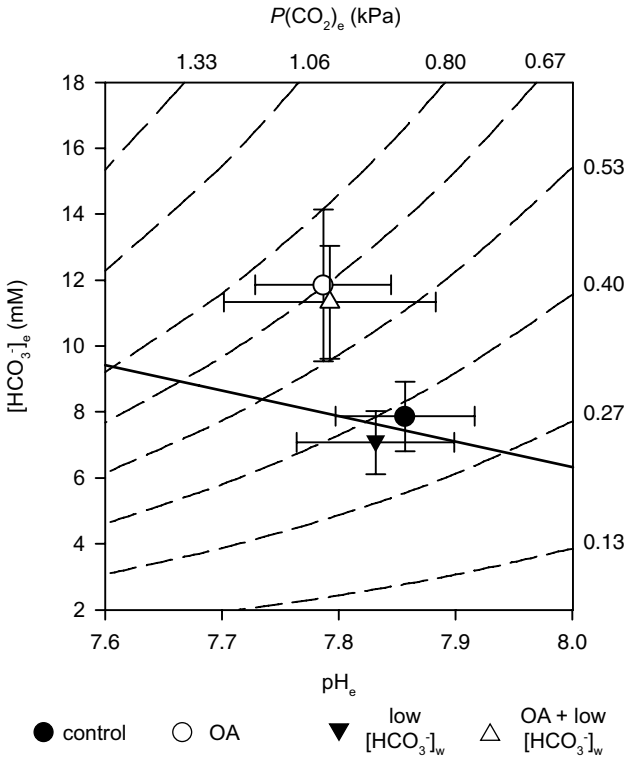

Fig. 5 pH/bicarbonate diagram representing acid–base status of the haemolymph of *C. maenas*. Values are group means ± standard deviation. Dashed lines represent isopleths for $P(CO_2)_e$. The solid, straight line represents the non-bicarbonate buffer value in the haemolymph, with the slope calculated as $\Delta[HCO_3^-]_e \cdot \Delta pH_e^{-1} = -7.7158$, after Truchot (1976). $P(CO_2)_e$ under OA is significantly higher than under low $[HCO_3^-]_w$ (ANOVA on ranks, $P < 0.05$). $[HCO_3^-]_e$ in both OA groups are significantly elevated above those in controls and under low $[HCO_3^-]_w$ (ANOVA on ranks, $P < 0.05$). Control: $n = 6$; OA: $n = 5$; low $[HCO_3^-]_w$: $n = 6$; OA + low $[HCO_3^-]_w$: $n = 4$. $T_w = 8$ °C. Data points are means ± SD

low $[HCO_3^-]_w$, indicating reduced motor activity or relaxed muscle tone. Low blood flow in the arteria sternalis could also mirror low energy demand of the walking leg muscle (McGaw et al. 1994). Limited crab movement during blood-flow measurements in the MRI scanner also argues for enhanced relaxation and reduced muscle tone under OA + low $[HCO_3^-]_w$.

The fact that the two hypercapnic groups experience the lowest pH_w (Table 1), and show the largest difference in physiological responses, emphasizes the importance of divergent carbonate alkalinities (and thus $[HCO_3^-]_w$). It seems unlikely that pH_w alone causes the diverging metabolic responses between OA and OA + low $[HCO_3^-]_w$: the difference in pH_w between these two groups was only 0.3 units, whereas between low $[HCO_3^-]_w$ and OA + low $[HCO_3^-]_w$ conditions, the difference was 0.7 units. SMR and blood-flow rates were similar in the two groups at reduced water bicarbonate levels, despite the larger pH_w difference between these groups. We thus conclude that changes in water bicarbonate levels are key in modulating the effects of OA on the metabolic and other responses of *C. maenas*.

We could not detect differences in steady-state heart rates between any of the treatments. Possible effects of shifting environmental parameters may be hidden in the intermittent and variable activity of the heart in *C. maenas* (Cumberlidge and Uglow 1977). For example, the measurements of blood flow and heart rate likely include phases of high (spMR) or low (SMR) metabolic activity (see Fig. 1). This might explain the large standard deviation of heart- and blood-flow rates over time especially under control conditions (Fig. 3e). Unraveling any effects of water parameters on the duration, frequency and amplitude of phases of depressed heart rate would require continuous recordings of heart activity. At constant heart rate, the observed reduction in flow rates at low $[HCO_3^-]_w$ should thus result from a reduction in stroke volume, in line with the observation that this parameter is

Table 2 Ion concentrations in the haemolymph

Ion	Control	OA	low $[HCO_3^-]_w$	OA + low $[HCO_3^-]_w$
Na^+	497 ± 33	533 ± 18*	525.7 ± 8.9	540 ± 16*
K^+	12.7 ± 1.6	14.0 ± 1.4	15.0 ± 2.3	12.4 ± 1.0
Mg^{2+}	21.6 ± 3.0	29.3 ± 4.8**	27.5 ± 3.3**	32.0 ± 1.7***
Ca^{2+}	11.3 ± 1.3	12.93 ± 0.48*	12.25 ± 0.65	13.21 ± 0.94*
Total cations	543 ± 39	589 ± 25	580 ± 15	597 ± 20
Cl^-	452 ± 19	445 ± 28	416 ± 20*	473 ± 22
HCO_3^-	7.9 ± 1.1	11.8 ± 2.3***	7.08 ± 0.96	11.3 ± 1.7**
Total ions	1003 ± 59	1046 ± 55	1003 ± 36	1082 ± 43

Concentrations given in mM. Total concentrations are the sum of group means. Control: $n = 7$; OA: $n = 5$; low $[HCO_3^-]_w$: $n = 5$; OA + low $[HCO_3^-]_w$: $n = 4$. For T_w and S, see Table 1. The numbers of asterisks indicate significant differences to the control group at various levels of significance (ANOVA, $*P < 0.05$, $**P < 0.01$, $***P < 0.001$). $[Ca^{2+}]$ in both OA groups are significantly higher than under normocapnic low $[HCO_3^-]_w$. $[Cl^-]$ content under normocapnic low $[HCO_3^-]_w$ is also significantly lower than under OA + low $[HCO_3^-]_w$

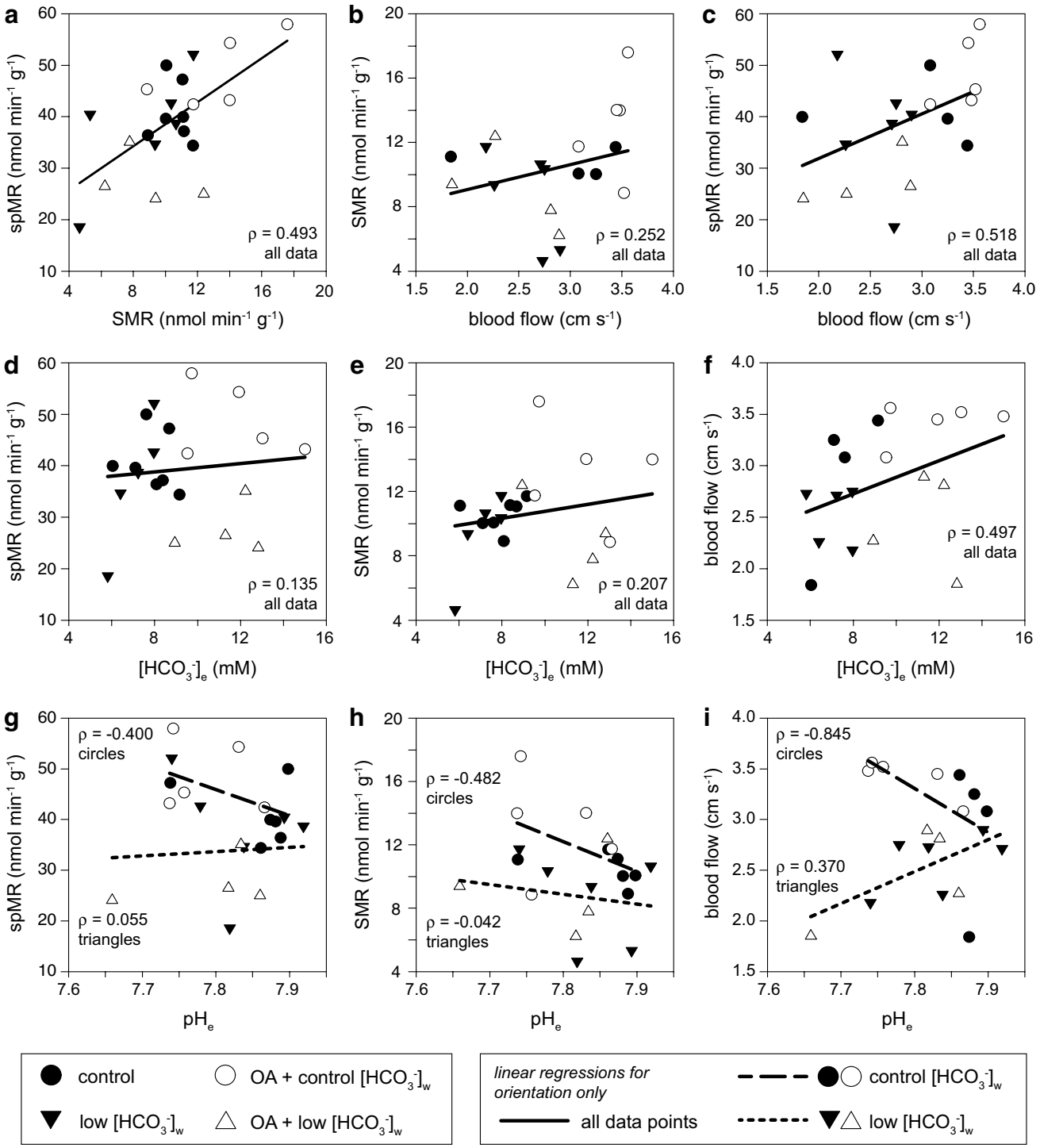

Fig. 6 Correlations between metabolic rates, blood-flow rates, $[HCO_3^-]_e$ and pH_e. Symbols represent individuals of the groups. Spearman rank correlation tests revealed significant correlations between spMR and SMR (**a**; $\rho = 0.493$, $P < 0.05$, $n = 22$); spMR and blood flow (**c**; $\rho = 0.518$, $P < 0.05$, $n = 19$), blood flow and haemolymph $[HCO_3^-]$ (**f**; $\rho = 0.497$, $P < 0.05$, $n = 18$). The correlation between blood flow and pH_e is only significant under control levels of water bicarbonate (**i**, open and closed circles; $\rho = -0.845$, $P < 0.001$, $n = 9$). Correlations in **b**, **d** and **e** were not significant, **g** and **h** showed only a negative correlation between blood flow and pH_e. Spearman's ρ is given in each panel. Lines are linear regressions for orientation only

most plastic in crustaceans (Taylor 1982). The mechanisms linking hypercapnia to cardiac function clearly require further investigations. Hypercapnia may constrain cardiac capacity and thereby lead to a reduction in oxygen uptake. In fact, haemolymph oxygen levels were lowered in crabs under $P(CO_2)_w = 3000$ µatm (Walther et al. 2009).

Acid–base-, metabolic, and ionic regulation

Control values for pH_i, pH_e, $P(CO_2)_e$, and $[HCO_3^-]_e$ are in good agreement with published values (Truchot 1973, 1981, 1984; Wheatly and Henry 1992; Appelhans et al. 2012; Fehsenfeld and Weihrauch 2016). Extracellular pH was fully compensated for through elevation of $[HCO_3^-]_e$, despite an increase of $P(CO_2)_e$. Our finding of efficient pH regulation during prolonged exposure to hypercapnia is in line with findings in other crustaceans ($P(CO_2)_w = 10{,}000$ µatm for *M. magister*, Pane and Barry 2007; $P(CO_2)_w = 2500$ µatm for *N. puber*, Spicer et al. 2007; $P(CO_2)_w = 3500$ µatm for *C. maenas*, Appelhans et al. 2012).

Full pH compensation after 4 weeks was found even under reduced levels of bicarbonate in the water (Fig. 5). Acid–base regulation after 4 weeks of incubation may in fact be more efficient than during acute exposure to altered seawater physicochemistry (e.g., Truchot 1984) and may reflect medium-term acclimation of compensatory mechanisms: neither moderate levels of hypercapnia, nor reduced $[HCO_3^-]_w$ or pH_w, nor combined exposures were found to induce an acidosis during medium-term exposure, indicating sufficiently high capacities of associated ion-exchange mechanisms in *C. maenas*. Nevertheless, animals still showed a 30% reduction in SMR and a 40% reduction in spMR after 4 weeks of exposure, despite full compensation of any transient changes in pH_e (and pH_i; Figs. 2, 4). Previous studies have indicated a role for reduced pH_e values in the onset of metabolic depression in a lower invertebrate (Reipschläger and Pörtner 1996; Pörtner et al. 1998). In our study, at unchanged pH_e values in all groups, the drop in metabolic rate may rather be attributed to the water carbonate system, potentially mediating its own, previously unreported effect on metabolic regulation of the shore crab.

At constant pH_e and elevated $P(CO_2)_e$, an increase of $[HCO_3^-]_e$ would occur as part of the compensation process, resulting from both, a potential uptake of bicarbonate from the seawater through Cl^-/HCO_3^- exchange or metabolic bicarbonate formation due to the release of protons or acid equivalents to the seawater (such as NH_4^+; Fehsenfeld and Weihrauch 2013). Proton equivalent ion exchange may help elevate $[HCO_3^-]_e$ well above the non-bicarbonate buffer line (Fig. 5; Fehsenfeld and Weihrauch 2013). Reducing $[HCO_3^-]_w$ will likely affect ion gradients and membrane potentials over apical membranes. Fehsenfeld and Weihrauch suggested that acid–base regulation mechanisms are flexible to compensate for variable sea- or brackish water alkalinity, e.g., through enhanced ammonium excretion (see Fehsenfeld and Weihrauch 2016a for a detailed description).

All treatments with acidified seawater led to increased cation concentrations in the haemolymph, involving significant increases in $[Mg^{2+}]$ and $[Na^+]$ above control values, comparable to findings in the Dungeness crab *M. magister* (Hans et al. 2014) and velvet crab *N. puber* (Spicer et al. 2007; Small et al. 2010). The increase of $[Na^+]$ at mostly unaffected or even reduced $[Cl^-]$ may indicate the relative involvement of Na^+/H^+ and Cl^-/HCO_3^- exchanges in pH_e regulation. This net effect might develop during longer term rather than acute exposures to ocean acidification. Accumulation of non-carbonate anions, such as SO_4^{2-} or negatively charged amino acids, might then be a way to compensate for the apparent lack of negative charges, especially at normocapnic low $[HCO_3^-]_w$ (Hammer et al. 2012; Hans et al. 2014). However, this is far beyond the scope of this study and needs further confirmation. The increase in extracellular SID observed in all treatments with altered seawater physicochemistry might thus reflect the successful compensation of the extracellular acidosis (Stewart 1978; Fencl and Leith 1993).

Feedback of seawater variables on metabolic rate and scope

Inter-individual variability, enhanced by a consistent effect of experimental conditions, is indicated by the significant correlation of metabolic rates (SMR, spMR; Fig. 6a), leading to invariable factorial aerobic scopes at variable absolute aerobic scopes (Fig. 2b). Since blood flow in the sternal artery is strongly correlated with spMR and less with SMR, we conclude, that cardiovascular activity parallels excess energy demand during phases of spontaneous activity (Fig. 6b, c). At the same time, high SMR and blood-flow support elevated spMR. Blood flow usually parallels the energy demand of tissues especially during spontaneous activity (Hamann et al. 2005), indicating that the energy demand of leg muscles may be lower under OA + low $[HCO_3^-]_w$ than under OA alone (see above). As a note of precaution, blood flow through the arteria sternalis does not necessarily mirror flow through the gills (Bock et al. 2001a), which could change independently to match altered energy demand of branchial ion-exchange processes, as shown, e.g., under salinity changes (Welcomme and Devos 1991; Kotlyar et al. 2000).

Further correlations are more obscure (Fig. 6d–i). The significant positive correlation between blood flow in the arteria sternalis and haemolymph $[HCO_3^-]$ (Fig. 6f) would indicate that high haemolymph $[HCO_3^-]$ in response to OA supports a stimulation of spontaneous metabolic rate (Fig. 2a). However, haemolymph $[HCO_3^-]$ is not correlated

with metabolic rates (Fig. 6d, e), as discussed above, pointing to water bicarbonate as the crucial difference. Responses to OA may thus become constrained by low $[HCO_3^-]_w$ (triangles in Fig. 6c). pH_e varied slightly with haemolymph bicarbonate (Fig. 5) and the correlation of pH_e with metabolic rates was less expressed between experimental groups (Fig. 6g, h). The strongest correlation here again was seen between pH_e and blood flow. The negative slope of this relationship (Fig. 6i) was lost or reversed into the opposite direction (Fig. 6i) at reduced water bicarbonate levels. Beyond direct feedbacks of pH_e on metabolic rate as reported in *S. nudus* (Pörtner et al. 2000) or *M. edulis* (Michaelidis et al. 2005), more complex relationships may involve a role for water bicarbonate levels under OA causing a shift in energy budget of the shore crab.

Finally, the complex relations between the physiological parameters investigated make a differentiated picture of the influence of seawater parameters on metabolic rate difficult. Further detailed studies of the responses of specific ion-exchange processes to different water acid–base conditions may help to unravel how the apparent capacities of acid–base regulation in *C. maenas* (cf. Fehsenfeld and Weihrauch 2016) influence metabolic rate and scope. While the energy demand of branchial ion exchangers such as Na^+/K^+-ATPase and V-type ATPase under OA has been studied in deep-sea crabs *Xenograpsus testudinatus* (Hu et al. 2016), similar measurements in intertidal *C. maenas* could shed more light on the energetic implications of changes in water bicarbonate levels at the whole-animal level. Here, the potential presence of mechanisms sensing water carbonate chemistry, as suggested for crayfish (Larimer 1964), could be of interest.

Conclusion and perspectives

After 1 month of exposure, *C. maenas* was found to tolerate OA beyond projected end-century conditions. At high ambient $P(CO_2)$, elevated blood $P(CO_2)$ was balanced by an increase of $[HCO_3^-]_e$, irrespective of seawater bicarbonate concentrations and supporting full compensation of pH_e and pH_i. These patterns may reflect long-term acclimation in acid–base regulation. However, despite constant pH_e and pH_i, whole-animal metabolic rates and blood-flow rates showed some variability. The reduction in metabolic scope and increased ratios of cellular PLA over inorganic phosphate levels at OA combined with low $[HCO_3^-]_w$ demonstrate energetic savings under fully aerobic conditions. Metabolic rates and blood-flow rates showed different correlations with pH_e at different water bicarbonate concentrations, which is a new observation. The mechanisms behind remain obscure but should be considered in future studies of the physiological responses of crustaceans to ocean acidification, under variable combinations of water $P(CO_2)$, $[HCO_3^-]$ and pH.

Acknowledgements The authors thank Fredy Veliz Moraleda and Silvia Hardenberg for assistance in animal maintenance. We thank Dr. Franz-Josef Sartoris for expertise on ion chromatography, Timo Hirse for assistance with the GC and Rolf Wittig for post-processing the MR data. We would like to thank three anonymous reviewers for their helpful comments, improving the manuscript.

Author contributions BM, CB and HP conceived and designed the experiments, and wrote and drafted the manuscript. BM carried out the experiments, with help from CB on MR experiments. BM performed the statistical analyses. All authors approved the final version of the manuscript.

Funding The study is a contribution to the PACES II research program (WP 1.6) of the Alfred Wegener Institute, funded by the Helmholtz Association.

Compliance with ethical standards

Conflict of interest No competing interests declared.

References

Appelhans YS, Thomsen J, Pansch C et al (2012) Sour times: seawater acidification effects on growth, feeding behaviour and acid–base status of *Asterias rubens* and *Carcinus maenas*. Mar Ecol Prog Ser 459:85–97. https://doi.org/10.3354/meps09697

Belman BW (1975) Some aspects of the circulatory physiology of the spiny lobster *Panulirus interruptus*. Mar Biol 29:295–305. https://doi.org/10.1007/BF00388849

Bock C, Frederich M, Wittig R-M, Pörtner H-O (2001a) Simultaneous observations of haemolymph flow and ventilation in marine spider crabs at different temperatures: a flow weighted MRI study. Magn Reson Imaging 19:1113–1124. https://doi.org/10.1016/S0730-725X(01)00414-3

Bock C, Sartoris F-J, Wittig R-M, Pörtner H-O (2001b) Temperature-dependent pH regulation in stenothermal Antarctic and eurythermal temperate eelpout (Zoarcidae): an in-vivo NMR study. Polar Biol 24:869–874. https://doi.org/10.1007/s003000100298

Bock C, Sartoris F-J, Pörtner H-O (2002) In vivo MR spectroscopy and MR imaging on non-anaesthetized marine fish: techniques and first results. Magn Reson Imaging 20:165–172. https://doi.org/10.1016/S0730-725x(02)00482-4

Bock C, Dogan F, Pörtner H-O (2012) Cardiovascular performance of the edible crap *Cancer pagurus* under the effects of ocean acidification. In: The ocean in a high-CO_2 world: third symposium. Monterey, CA, USA

Bohning DE, Carter B, Liu S, Pohost GM (1990) PC-Based system for retrospective cardiac and respiratory gating of NMR data. Magn Reson Med 16:303–316. https://doi.org/10.1002/mrm.1910160211

Boutilier RG, Heming TA, Iwama GK (1984) Appendix: physicochemical parameters for use in fish respiratory physiology. In: Hoar WS, Randall DJ (eds) Fish physiology. Elsevier, Amsterdam, pp 403–430

Brand MD (1990) The Contribution of the leak of protons across the mitochondrial inner membrane to standard metabolic rate. J Theor Biol 145:267–286

Charmantier G, Charmantier-Daures M, Towle DW (2009) Osmoic and ionic regulation in aquatic arthropods. In: Evans DH (ed) Osmotic and ionic regulation—calls and animals. CRC Press, Boca Raton, pp 165–230

Clark TD, Sandblom E, Jutfelt F (2013) Aerobic scope measurements of fishes in an era of climate change: respirometry, relevance and recommendations. J Exp Biol 216:2771–2782. https://doi.org/10.1242/jeb.084251

Cumberlidge N, Uglow RF (1977) Heart and scaphognathite activity in the shore crab *Carcinus maenas* (L.). J Exp Mar Bio Ecol 28:87–107. https://doi.org/10.1016/0022-0981(77)90065-X

Dejours P (1981) Principles of comparative respiratory physiology, 2nd edn. Elsevier/North-Holland Biomedical Press, Amsterdam

Dickson AG (1990) Standard potential of the reaction: AgCl(s) + 1/2H_2(g) = Ag(s) + HCl(aq), and the standard acidity constant of the ion HSO_4—in synthetic sea water from 273.15 to 318.15 K. J Chem Thermodyn 22:113–127. https://doi.org/10.1016/0021-9614(90)90074-Z

Dickson AG (2010) The carbon dioxide system in seawater: equilibrium chemistry and measurements. In: Riebesell U, Fabry VJ, Hansson L, Gattuso J-P (eds) Guide to best practices in ocean acidification research and data reporting. European Comission, Directorate-General for Research, Brussels, pp 17–40

Doney SC, Fabry VJ, Feely RA, Kleypas JA (2009) Ocean acidification: the other CO_2 problem. Ann Rev Mar Sci 1:169–192. https://doi.org/10.1146/annurev.marine.010908.163834

Dupont-Prinet A, Chatain B, Grima L et al (2010) Physiological mechanisms underlying a trade-off between growth rate and tolerance of feed deprivation in the European sea bass (*Dicentrarchus labrax*). J Exp Biol 213:1143–1152. https://doi.org/10.1242/jeb.037812

Fabry VJ, Seibel BA, Feely RA, Orr JC (2008) Impacts of ocean acidification on marine fauna and ecosystem processes. ICES J Mar Sci 65:414–432. https://doi.org/10.1093/icesjms/fsn048

Fehsenfeld S, Weihrauch D (2013) Differential acid–base regulation in various gills of the green crab *Carcinus maenas*: effects of elevated environmental pCO_2. Comp Biochem Physiol A 164:54–65. https://doi.org/10.1016/j.cbpa.2012.09.016

Fehsenfeld S, Weihrauch D (2016) Mechanisms of acid–base regulation in seawater-acclimated green crabs (*Carcinus maenas*). Can J Zool 107:95–107

Fencl V, Leith DE (1993) Stewart's quantitative acid–base chemistry: applications in biology and medicine. Respir Physiol 91:1–16. https://doi.org/10.1016/0034-5687(93)90085-O

Fernández M, Bock C, Pörtner H-O (2000) The cost of being a caring mother: the ignored factor in the reproduction of marine invertebrates. Ecol Lett 3:487–494. https://doi.org/10.1046/j.1461-0248.2000.00172.x

Frederich M, Pörtner H-O (2000) Oxygen limitation of thermal tolerance defined by cardiac and ventilatory performance in spider crab, Maja squinado. Am J Physiol Regul Integr Comp Physiol 279:R1531–R1538

Fry FEJ (1971) The effect of environmental factors on the physiology of fish. In: Hoar WS, Randall DJ (eds) Fish physiology. Academic Press, New York, pp 1–98

Gillies RJ, Liu Z, Bhujwalla Z (1994) 31P-MRS measurements of extracellular pH of tumors using 3-aminopropylphosphonate. Am J Physiol 267:C195–C203

Guppy M, Withers P (1999) Metabolic depression in animals: physiological perspectives and biochemical generalizations. Biol Rev Camb Philos Soc 74:1–40

Gutowska MA, Pörtner H-O, Melzner F (2008) Growth and calcification in the cephalopod *Sepia officinalis* under elevated seawater pCO_2. Mar Ecol Prog Ser 373:303–309. https://doi.org/10.3354/meps07782

Gutowska MA, Melzner F, Langenbuch M et al (2010) Acid–base regulatory ability of the cephalopod (*Sepia officinalis*) in response to environmental hypercapnia. J Comp Physiol B 180:323–335. https://doi.org/10.1007/s00360-009-0412-y

Hamann JJ, Kluess HA, Buckwalter JB, Clifford PS (2005) Blood flow response to muscle contractions is more closely related to metabolic rate than contractile work. J Appl Physiol 98:2096–2100. https://doi.org/10.1152/japplphysiol.00400.2004

Hammer KM, Pedersen SA, Strøseth TR (2012) Elevated seawater levels of CO_2 change the metabolic fingerprint of tissues and hemolymph from the green shore crab *Carcinus maenas*. Comp Biochem Physiol Part D Genom Proteom 7:292–302. https://doi.org/10.1016/j.cbd.2012.06.001

Hans S, Fehsenfeld S, Treberg JR, Weihrauch D (2014) Acid–base regulation in the Dungeness crab (*Metacarcinus magister*). Mar Biol 161:1179–1193. https://doi.org/10.1007/s00227-014-2409-7

Heisler N (ed) (1986) Acid–base regulation in animals. Elsevier, Amsterdam

Henry RP, Lucu C, Onken H, Weihrauch D (2012) Multiple functions of the crustacean gill: osmotic/ionic regulation, acid–base balance, ammonia excretion, and bioaccumulation of toxic metals. Front Physiol 3:1–33. https://doi.org/10.3389/fphys.2012.00431

Hu MY, Guh YJ, Shao YT et al (2016) Strong ion regulatory abilities enable the crab *Xenograpsus testudinatus* to inhabit highly acidified marine vent systems. Front Physiol 7:1–11. https://doi.org/10.3389/fphys.2016.00014

Hu MY, Tseng Y-C, Su Y-H et al (2017) Variability in larval gut pH regulation defines sensitivity to ocean acidification in six species of the *Ambulacraria superphylum*. Proc Biol Sci 284:20171066. https://doi.org/10.1098/rspb.2017.1066

Klein Breteler WCM (1975) Oxygen consumption and respiratory levels of juvenile shore crabs, *Carcinus maenas*, in relation to weight and temperature. Neth J Sea Res 9:243–254

Kleps RA, Myers TC, Lipdus RN, Henderson TO (2007) A sex-specific metabolite identified in a marine invertebrate utilizing phosphorus-31 nuclear magnetic resonance. PLoS One 2:e780. https://doi.org/10.1371/journal.pone.0000780

Kotlyar S, Weihrauch D, Paulsen RS, Towle DW (2000) Expression of arginine kinase enzymatic activity and mRNA in gills of the euryhaline crabs *Carcinus maenas* and *Callinectes sapidus*. J Exp Biol 203:2395–2404

Kreiß C (2010) Simultane Quantifizierung von extra- und intrazellulären pH-Werten bei *Carcinus maenas* unter CO_2-*Einfluss mittels* in vivo 31P-NMR. University Bremen, Bremen

Kreiß C, Michael K, Lucassen M et al (2015) Ocean warming and acidification modulate energy budget and gill ion regulatory mechanisms in Atlantic cod (*Gadus morhua*). J Comp Physiol B. https://doi.org/10.1007/s00360-015-0923-7

Larimer JL (1964) Sensory-induced modifications of ventilation and heart rate in crayfish. Comp Biochem Physiol 12:25–36. https://doi.org/10.1016/0010-406X(64)90045-3

Linnaeus C (1758) Systema naturae per regna tria naturae, secundum classes, ordines, genera, species, cum characteribus, differentiis, synonymis, locis, editio decima, reformata, vol ii. Laurentius Salvius, Holmiae, p 824

McGaw IJ, Penney CM (2014) Effect of meal type on specific dynamic action in the green shore crab, *Carcinus maenas*. J Comp Physiol B 184:425–436. https://doi.org/10.1007/s00360-014-0812-5

McGaw IJ, Airriess CN, McMahon BR (1994) Patterns of haemolymph-flow variation in decapod crustaceans. Mar Biol 121:53–60. https://doi.org/10.1007/BF00349473

Meinshausen M, Smith SJ, Calvin K et al (2011) The RCP greenhouse gas concentrations and their extensions from 1765 to 2300. Clim Chang 109:213–241. https://doi.org/10.1007/s10584-011-0156-z

Michael K, Kreiß C, Hu MY et al (2016) Adjustments of molecular key components of branchial ion and pH regulation in Atlantic cod

(*Gadus morhua*) in response to ocean acidification and warming. Comp Biochem Physiol Part B Biochem Mol Biol 193:33–46. https://doi.org/10.1016/j.cbpb.2015.12.006

Michaelidis B, Ouzounis C, Paleras A, Pörtner H-O (2005) Effects of long-term moderate hypercapnia on acid–base balance and growth rate in marine mussels *Mytilus galloprovincialis*. Mar Ecol Prog Ser 293:109–118. https://doi.org/10.3354/meps293109

Millero FJ (2010) Carbonate constants for estuarine waters. Mar Freshw Res 61:139. https://doi.org/10.1071/MF09254

Pane EF, Barry JP (2007) Extracellular acid–base regulation during short-term hypercapnia is effective in a shallow water crab, but ineffective in a deep-sea crab. Mar Ecol Prog Ser 334:1–9. https://doi.org/10.3354/meps334001

Pierrot D, Lewis E, Wallace DWR (2006) MS excel program developed for CO_2 system calculations. ORNL/CDIAC-105a. Carbon Dioxide Information Analysis Center, Oak Ridge National Laboratory, U.S. Department of Energy, Oak Ridge, Tennessee. https://doi.org/10.3334/CDIAC/otg.CO2SYS_XLS_CDIAC105a

Pope JM, Yao S (1993) Quantitative NMR imaging of flow. Concepts Magn Reson 5:281–302. https://doi.org/10.1002/cmr.1820050402

Pörtner H-O, Boutilier RG, Tang Y, Toews DP (1990) Determination of intracellular pH and PCO_2 after metabolic inhibiton by fluoride and nitrilotriacetic acid. Respir Physiol 81:255–273. https://doi.org/10.1016/0034-5687(90)90050-9

Pörtner H-O, Reipschläger A, Heisler N (1998) Acid–base regulation, metabolism and energetics in *Sipunculus nudus* as a function of ambient carbon dioxide level. J Exp Biol 201:43–55

Pörtner H-O, Bock C, Reipschläger A (2000) Modulation of the cost of pHi regulation during metabolic depression: a 31P-NMR study in invertebrate (*Sipunculus nudus*) isolated muscle. J Exp Biol 203:2417–2428

Pörtner H-O, Langenbuch M, Reipschläger A (2004) Biological impact of elevated CO_2 concentrations: lessons from animal physiology and earth history? J Oceanogr 60:705–718

Pörtner H-O, Bickmeyer U, Bleich M et al (2010) Studies of acid–base status and regulation. In: Riebesell U, Fabry VJ, Hansson L, Gattuso J-P (eds) Guide to best practices in ocean acidification research and data reporting. European Comission, Directorate-General for Research, Brussels, pp 137–166

Reipschläger A, Pörtner H-O (1996) Metabolic depression during environmental stress: the role of extracellular versus intracellular pH in *Sipunculus nudus*. J Exp Biol 199:1801–1807

Robertson RF, Meagor J, Taylor EW (2002) Specific dynamic action in the shore crab, *Carcinus maenas* (L.), in relation to acclimation temperature and to the onset of the emersion response. Physiol Biochem Zool 75:350–359. https://doi.org/10.1086/342801

Small D, Calosi P, White D et al (2010) Impact of medium-term exposure to CO_2 enriched seawater on the physiological functions of the velvet swimming crab *Necora puber*. Aquat Biol 10:11–21. https://doi.org/10.3354/ab00266

Sokolova IM, Bock C, Pörtner H-O (2000) Resistance to freshwater exposure in White Sea Littorina spp. I: anaerobic metabolism and energetics. J Comp Physiol B 170:91–103. https://doi.org/10.1007/s003600050264

Spicer JI, Raffo A, Widdicombe S (2007) Influence of CO_2-related seawater acidification on extracellular acid–base balance in the velvet swimming crab *Necora puber*. Mar Biol 151:1117–1125. https://doi.org/10.1007/s00227-006-0551-6

Steffensen JF (1989) Some errors in respirometry of aquatic breathers: how to avoid and correct for them. Fish Physiol Biochem 6:49–59. https://doi.org/10.1007/BF02995809

Stewart PA (1978) Independent and dependent variables of acid–base control. Respir Physiol 33:9–26. https://doi.org/10.1016/0034-5687(78)90079-8

Taylor EW (1982) Control and co-ordination of ventilation and circulation in crustaceans: responses to hypoxia and exercise. J Exp Biol 100:289–319

Tepolt CK, Somero GN (2014) Master of all trades: thermal acclimation and adaptation of cardiac function in a broadly distributed marine invasive species, the European green crab, *Carcinus maenas*. J Exp Biol 217:1129–1138. https://doi.org/10.1242/jeb.093849

Thomsen J, Melzner F (2010) Moderate seawater acidification does not elicit long-term metabolic depression in the blue mussel *Mytilus edulis*. Mar Biol 157:2667–2676. https://doi.org/10.1007/s00227-010-1527-0

Thomsen J, Gutowska MA, Saphörster J et al (2010) Calcifying invertebrates succeed in a naturally CO_2-rich coastal habitat but are threatened by high levels of future acidification. Biogeosciences 7:3879–3891. https://doi.org/10.5194/bg-7-3879-2010

Truchot J-P (1973) Temperature and acid–Base Regulation in the Shore Crab. Respir Physiol 17:11–20

Truchot J-P (1976) Carbon dioxide combining properties of the blood of the shore crab, *Carcinus maenas* (L.): CO_2-dissociation curves and Haldane effect. J Comp Physiol B 112(3):283–293

Truchot J-P (1979) Mechanisms of the compensation of blood respiratory acid–base disturbances in the shore crab, *Carcinus maenas* (L.). J Exp Zool 210:407–416. https://doi.org/10.1002/jez.1402100305

Truchot J-P (1981) The effect of water salinity and acid–base state on the blood acid–base balance in the eryhaline crab, *Carcinus maenas* (L.). Comp Biochem Physiol A 68:555–561

Truchot J-P (1984) Water carbonate alkalinity as a determinant of hemolymph acid–base balance in the shore crab, *Carcinus maenas*: a study at two different ambient PCO_2 and PO_2 levels. J Comp Physiol B 154:601–606. https://doi.org/10.1007/BF00684414

Uppström LR (1974) The boron/chlorinity ratio of deep-sea water from the Pacific Ocean. Deep Sea Res Oceanogr Abstr 21:161–162. https://doi.org/10.1016/0011-7471(74)90074-6

Walther K, Sartoris F-J, Bock C, Pörtner H-O (2009) Impact of anthropogenic ocean acidification on thermal tolerance of the spider crab *Hyas araneus*. Biogeosci Discuss 6:2837–2861. https://doi.org/10.5194/bgd-6-2837-2009

Waters JF, Millero FJ (2013) The free proton concentration scale for seawater pH. Mar Chem 149:8–22. https://doi.org/10.1016/j.marchem.2012.11.003

Welcomme L, Devos P (1991) Energy consumption in the perfused gills of the euryhaline crab Eriocheir sinensis [H. Miln. Edw.] adapted to freshwater. J Exp Zool 257:150–159. https://doi.org/10.1002/jez.1402570203

Wheatly MG (1985) The role of the antennal gland in ion and acid–base regulation during hyposaline exposure of the Dungeness crab *Cancer magister* (Dana). J Comp Physiol B 155:445–454. https://doi.org/10.1007/BF00684674

Wheatly MG, Henry RP (1992) Extracellular and intracellular acid–base regulation in crustaceans. J Exp Zool 263:127–142. https://doi.org/10.1002/jez.1402630204

Whiteley NM (2011) Physiological and ecological responses of crustaceans to ocean acidification. Mar Ecol Prog Ser 430:257–271. https://doi.org/10.3354/meps09185

Wittmann AC (2010) Life in cold oceans: activity dependent on extracellular ion regulation? Die Rolle der extrazellulären Ionenregulation in der Kältetoleranz mariner Crustaceen. University Bremen, Bremen

Wittmann AC, Pörtner H-O (2013) Sensitivities of extant animal taxa to ocean acidification. Nat Clim Chang 3:995–1001. https://doi.org/10.1038/nclimate1982

Zange J, Grieshaber MK, Jans AW (1990) The Regulation of intracellular pH estimated by 31P-NMR spectroscopy in the anterior byssus retractor muscle of *Mytilus edulis* L. J Exp Biol 150:95–109